Xu G, Wang GZ. AHT Bézier curves and NUAHT B-spline curves. JOURNAL OF COMPUTER SCIENCE AND TECHNOLOGY 22(4): 597~607 July 2007

AHT Bézier Curves and NUAHT B-Spline Curves

Gang Xu (徐 岗) and Guo-Zhao Wang (汪国昭)

[1] *Institute of Computer Graphics and Image Processing, Zhejiang University, Hangzhou 310027, China*

[2] *Department of Mathematics, Zhejiang University, Hangzhou 310027, China*

E-mail: yln41@hotmail.com; wanggz@zju.edu.cn

Received February 21, 2006; revised December 20, 2006.

Abstract In this paper, we present two new unified mathematics models of conics and polynomial curves, called *algebraic hyperbolic trigonometric* (*AHT*) *Bézier curves* and *non-uniform algebraic hyperbolic trigonometric* (*NUAHT*) *B-spline curves of order n*, which are generated over the space $\mathrm{span}\{\sin t, \cos t, \sinh t, \cosh t, 1, t, \ldots, t^{n-5}\}$, $n \geqslant 5$. The two kinds of curves share most of the properties as those of the Bézier curves and B-spline curves in polynomial space. In particular, they can represent exactly some remarkable transcendental curves such as the helix, the cycloid and the catenary. The subdivision formulae of these new kinds of curves are also given. The generations of the tensor product surfaces are straightforward. Using the new mathematics models, we present the control mesh representations of two classes of minimal surfaces.

Keywords CAD/CAM, AHT Bézier curve, NUAHT B-spline curves, transcendental curves

1 Introduction

Curve and surface modeling is an important subject of computer graphics[1~3]. The rational Bézier scheme and the NURBS scheme have become de facto standards for the representation of curves and surfaces in CAGD, primarily because they encompass both freedom and traditional analytical shapes under a unified mathematical model[4~6]. However, Farin[7,8] and Piegl[9] also warned that the rational models introduce several drawbacks. For instance, their derivatives and integrals are hard to compute due to their rational forms. Furthermore, they cannot represent exactly transcendental curves such as the helix, the cycloid, the catenary and the exponential curve, which play a key role in engineering. In order to avoid the inconveniences of these schemes, finding new bases in new spaces seems to be the only way.

In this paper, we present two new unified mathematics models of conics and algebraic polynomial curves, called *algebraic hyperbolic trigonometric* (*AHT*) *Bézier curves* and *non-uniform algebraic hyperbolic trigonometric* (*NUAHT*) *B-spline curves of order n*, which are generated over the space $\mathrm{span}\{\sin t, \cos t, \sinh t, \cosh t, 1, t, \ldots, t^{n-5}\}$, $n \geqslant 5$. Such curves share most of the properties as those of the Bézier curves and B-spline curves in polynomial space. Furthermore, they can represent exactly some transcendental curves such as the helix, the cycloid and the catenary.

2 Related Work

In recent years, many bases are proposed in new space for geometric modeling in CAGD. Peña[10] constructed a basis for the space spanned by $\{1, \cos t, \ldots, \cos mt\}$. Zhang[11,12] investigated C-curves in the space $\mathrm{span}\{1, t, \cos t, \sin t\}$, which coincide with the H-curves[13]. Sânchez-Reyes[14] gave a basis of the space spanned by $\{1, \sin t, \cos t, \ldots, \sin mt, \cos mt\}$. Mainar *et al.*[15] found some B-bases for the spaces spanned by $\{1, t, \cos t, \sin t, \cos 2t, \sin 2t\}$, $\{1, t, t^2, \cos t, \sin t\}$, and $\{1, t, \cos t, \sin t, t\cos t, t\sin t\}$. Li[16] and Lü[17] *et al.* proposed the H-Bézier curves and the uniform hyperbolic polynomial B-spline curves in the space spanned by $\{\sinh t, \cosh t, 1, t, \ldots, t^{n-3}\}$. Chen *et al.*[18] and Wang *et al.*[19] constructed C-Bézier basis and the non-uniform algebraic trigonometric (NUAT) B-spline basis of the space spanned by $\{\sin t, \cos t, 1, t, \ldots, t^{n-3}\}$. However, the above curves are only able to represent exactly two kinds of conics at most. In other words, none of them are the unified mathematic model of conics, which keeps them from being applied conveniently in CAD/CAM.

In order to build a unified mathematic model of conics, Zhang *et al.*[20,21] unified C-curves and the H-curves by extending the calculation to complex numbers. However, trigonometric function and hyperbolic function cannot appear simultaneously in their models.

3 AHT Bézier Basis

3.1 Construction of AHT Bézier Basis

We first give four initial functions (see Fig.1(a))

$$B_{0,3}(t) = \frac{S(\alpha - t)}{S(\alpha)},$$

$$B_{1,3}(t) = \frac{C(\alpha - t)}{C(\alpha)} - \frac{S(\alpha - t)}{S(\alpha)},$$

$$B_{2,3}(t) = \frac{C(t)}{C(\alpha)} - \frac{S(t)}{S(\alpha)},$$

$$B_{3,3}(t) = \frac{S(t)}{S(\alpha)},$$

Regular Paper

This work is supported by the National Natural Science Foundation of China under Grant Nos. 60473130, 10371110 and the National Grand Fundamental Research 973 Program of China under Grant No. 2004CB318000.

where $S(t) = \sin t - \sinh t$, $C(t) = \cos t - \cosh t$, $t \in [0, \alpha]$, $\alpha \in (0, 3\pi/2]$.

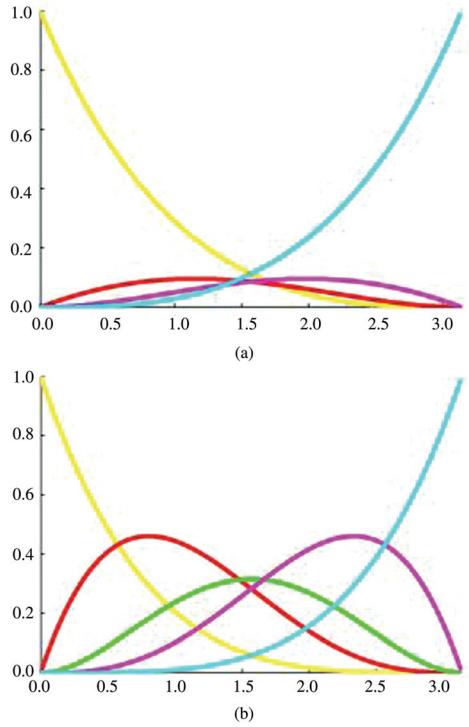

Fig.1. AHT Bézier basis. (a) Four initial functions with $\alpha = \pi$. (b) Case of order 5.

For $n > 3$, AHT Bézier basis functions $\{B_{0,n}, B_{1,n}, \ldots, B_{n,n}\}$ of the space $\Gamma_{n+1} = \text{span}\{\sin t, \cos t, \sinh t, \cosh t, 1, t, t^2, \ldots, t^{n-4}\}$ are defined recursively by (see Fig.1(b))

$$B_{0,n}(t) = 1 - \int_0^t \delta_{0,n-1} B_{0,n-1}(s)\mathrm{d}s,$$

$$B_{i,n}(t) = \int_0^t (\delta_{i-1,n-1} B_{i-1,n-1}(s) - \delta_{i,n-1} B_{i,n-1}(s))\mathrm{d}s, \quad 1 \leqslant i \leqslant n-1,$$

$$B_{n,n}(t) = \int_0^t \delta_{n-1,n-1} B_{n-1,n-1}(s)\mathrm{d}s,$$

where $\delta_{i,n} = 1 \Big/ \int_0^\alpha B_{i,n}(t)\mathrm{d}t$, $0 < i < n$.

3.2 Properties of AHT Bézier Basis

1) *Partition of Unity*: $\sum_{i=0}^n B_{i,n}(t) = 1$.
2) *Symmetry*: $B_{i,n}(t) = B_{n-i,n}(\alpha - t)$.
3) *Properties of the Endpoints*:

$$B_{0,n}(0) = B_{n,n}(\alpha) = 1, \quad B_{i,n}^{(j)}(0) = B_{i,n}^{(k)}(\alpha) = 0,$$

where $j = 0, 1, \ldots, i-1$, $k = 0, 1, \ldots, n-i-1$.

4) *Linear Independence*: $B_{0,n}, B_{1,n}, \ldots, B_{n,n}$ are linear independent and $\{B_{0,n}, B_{1,n}, \ldots, B_{n,n}\}$ is a basis of Γ_{n+1}.

5) *Degree-Elevation*:

$$B_{i,n}(t) = \frac{B_{i,n}^{(i)}(0)}{B_{i,n+1}^{(i)}(0)} B_{i,n+1}(t) + \left(1 - \frac{B_{i+1,n}^{(i+1)}(0)}{B_{i+1,n+1}^{(i)}(0)}\right) B_{i+1,n+1}(t).$$

We can prove it with the same method as those of the C-Bézier basis[15].

6) *Positivity*: $B_{i,n}(t) > 0$ for $t \in (0, \alpha)$, so AHT Bézier basis is a blending system.

The proof of the positivity is based on the following lemmas.

Lemma 3.1. *Let $\alpha \in (0, 3\pi/2]$ and $f(t) = a\cos t + b\sin t + c\sinh t + d\cosh t$, then $f(t)$ has at most four zeros on $[0, \alpha]$, where $a, b, c, d \in \mathbb{R}$ and they are all not equal to zero.*

Proof. Using proof by contradiction, we can prove it from the Rolle's Theorem. □

Lemma 3.2. *$B_{i,n}(t)$ has and only has n zeros on $[0, \alpha]$, $\alpha \in (0, 3\pi/2]$, $n \geqslant 4$.*

Proof. Using proof by contradiction, we can prove it from Lemma 3.1, the property 3) and Rolle's Theorem. □

Proposition 3.1. *$B_{i,n}(t) > 0$ for $t \in (0, \alpha)$.*

Proof. From Lemma 3.2, we know that $B_{i,n}(t)$ has and only has n zeros at $[0, \alpha]$ including the i-fold zero at 0 and the $(n-i)$-fold zero at α, so $B_{i,n}(t)$ is either positive or negative on the interval $(0, \alpha)$. The proof is completed together with property 3). □

7) *The AHT Bézier Basis is B-Basis*: by the properties 1), 5) and 6), we have that AHT Bézier basis is a totally positive basis. It is easy to get $\inf\{B_{i,n}(t)/B_{j,n}(t) | B_{j,n}(t) \neq 0\} = 0$ by L'Hospital's Rule. From Proposition 3.12 in [22], AHT Bézier basis is B-basis, so it has optimal shape preserving properties and optimal stability properties for the evaluation[23].

4 AHT Bézier Curve and Its Applications

An AHT Bézier curve $\boldsymbol{p}(t)$ of order $n+1$ is defined by

$$\boldsymbol{p}(t) = \sum_{i=0}^n B_{i,n}(t)\boldsymbol{P}_i, \quad t \in [0, \alpha],$$

where $\{B_{i,n}(t)\}_{i=0}^n$ is the AHT Bézier basis for the space Γ_{n+1}, $\boldsymbol{P}_i$ is the control point, and α is a global shape parameter, $\alpha \in (0, 3\pi/2]$.

4.1 Geometric Properties of the AHT Bézier Curves

1) *Endpoints Interpolation*:

$$\boldsymbol{p}(0) = \boldsymbol{P}_0, \quad \boldsymbol{p}(\alpha) = \boldsymbol{P}_n.$$

2) *Convex Hull Property*: the entire AHT Bézier curve $\boldsymbol{p}(t)$ must lie inside its control polygon spanned by $\boldsymbol{P}_0, \ldots, \boldsymbol{P}_n$.

3) *Derivative*: the derivative of $\boldsymbol{p}(t)$ is clearly a curve of order n:

$$\boldsymbol{p}'(t) = \sum_{i=0}^{n-1} B_{i,n-1}(t)\boldsymbol{Q}_i,\ t \in [0, \alpha],$$

where $\boldsymbol{Q}_i = \delta_{i,n-1}(\boldsymbol{P}_{i+1} - \boldsymbol{P}_i)$.

In particular, we have

$$\boldsymbol{p}^{(k)}(0) = \sum_{i=0}^{k} B_{i,n}^{(k)}(0)\boldsymbol{P}_i,$$

$$\boldsymbol{p}^{(k)}(\alpha) = \sum_{i=0}^{k} B_{i,n}^{(k)}(\alpha)\boldsymbol{P}_{n-i}.$$

4) *Degree-Elevation*:

$$\boldsymbol{p}(t) = \sum_{i=0}^{n} B_{i,n}(t)\boldsymbol{P}_i = \sum_{i=0}^{n+1} B_{i,n+1}(t)\boldsymbol{Q}_i. \qquad (1)$$

Here

$$\boldsymbol{Q}_0 = \boldsymbol{P}_0,$$

$$\boldsymbol{Q}_i = \Big(1 - \frac{B_{i,n}^{(i)}(0)}{B_{i,n+1}^{(i)}(0)}\Big)\boldsymbol{P}_{i-1} + \frac{B_{i,n}^{(i)}(0)}{B_{i,n+1}^{(i)}(0)}\boldsymbol{P}_i,\ i = 1, \ldots, n,$$

$$\boldsymbol{Q}_{n+1} = \boldsymbol{P}_n.$$

In fact, a degree-elevation procedure is a corner cutting procedure just as those of the Bézier curve. Using the method presented in [24], we can prove that the sequence of the control polygons that we get recursively from (1) converges to the AHT Bézier curve.

5) *Variation Diminishing Property*: no plane intersects an AHT Bézier curve more often than it intersects the corresponding control polygon.

6) *Convexity Preserving Property*: if the control polygon is convex, then the corresponding AHT Bézier curve is also convex.

We will prove the above two properties in Subsection 6.2.

7) *Limit of the AHT Bézier Curves*: as $\alpha \to 0$, the limit of an AHT Bézier curve in the space Γ_{n+1} approaches a Bézier curve in the space spanned by $\{1, t, t^2, \ldots, t^n\}$ (see Fig.2).

8) *Subdivision of the AHT Bézier Curves*: AHT Bézier curves admit a de Casteljau-type algorithm, called B-algorithm[25], that provides evaluation and subdivision. This property can also be derived via blossoming[13]. We will give the algorithm in Subsection 6.2 via inserting new knots. In fact, as $\alpha \to 0$, the B-algorithm reduces to the standard de Casteljau algorithm. This property is consistent with property 7) in this subsection.

9) *Critical Lengths for Design Purposes of* Γ_{n+1}: in [26], it was shown that certain spaces admit preserving representations on and only on compact intervals whose length is strictly less than a fixed value. This value depends only on the space and it is called the *critical length for design purposes*. For a given space of functions, the *critical length for design purposes* determines the supremum of the amplitudes of the interval, so that it is of interest in CAGD.

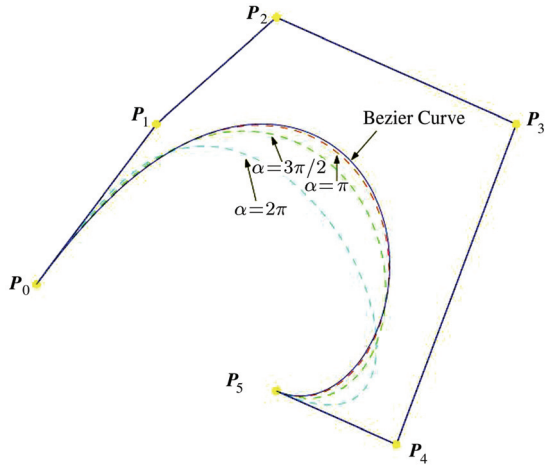

Fig.2. Limit of AHT Bézier curve.

Table 1 lists the critical lengths for design purposes of Γ_{n+1}, $n = 3, 4, 5, 6, 7, 8$.

Table 1. Critical Lengths for Design Purpose of Γ_{n+1}, $n = 3, 4, 5, 6, 7, 8$.

Space	Γ_4	Γ_5	Γ_6	Γ_7	Γ_8	Γ_9
Critical Length	1.5056π	1.5056π	2.4997π	2.4997π	3.1023π	3.1023π

4.2 Applications

In order to illustrate the practical value of the new mathematic model, we will represent some special curves and surfaces by quintic AHT Bézier basis in this subsection. We firstly present the transform matrix between $\{1, t, \sin t, \cos t, \sinh t, \cosh t\}$ and the quintic AHT Bézier basis $\{B_{i,5}\}_{i=0}^{5}$ as follows.

$$\begin{aligned}&(1, t, \sin t, \cos t, \sinh t, \cosh t)^{\top}\\ =&\boldsymbol{T}(B_{0,5}, B_{1,5}, B_{2,5}, B_{3,5}, B_{4,5}, B_{5,5})^{\top},\end{aligned}$$

where

$$\begin{aligned}\boldsymbol{T} =&(a_{ij})_{6\times 6}\\ =&\begin{pmatrix} 1 & 1 & 1 & 1 & 1 & 1\\ 0 & \delta & M & \alpha - M & \alpha - \delta & \alpha\\ 0 & \delta & M & Ns - Mc & s - \delta c & s\\ 1 & 1 & N & Nc + Ms & c + \delta s & c\\ 0 & \delta & M & L\bar{s} - M\bar{c} & \bar{s} - \delta\bar{c} & \bar{s}\\ 1 & 1 & L & L\bar{c} - M\bar{s} & \bar{c} - \delta\bar{s} & \bar{c}\end{pmatrix},\end{aligned} \qquad (2)$$

where

$$\begin{aligned}&F(t) = \frac{1}{2}(\sinh t + \sin t) - t,\\ &f_i = F^{(i)}(\alpha), \quad e = f_1^2 - f_0 f_2,\\ &g = f_0 f_3 - f_1 f_2, \quad h = f_2^2 - f_1 f_3,\end{aligned}$$

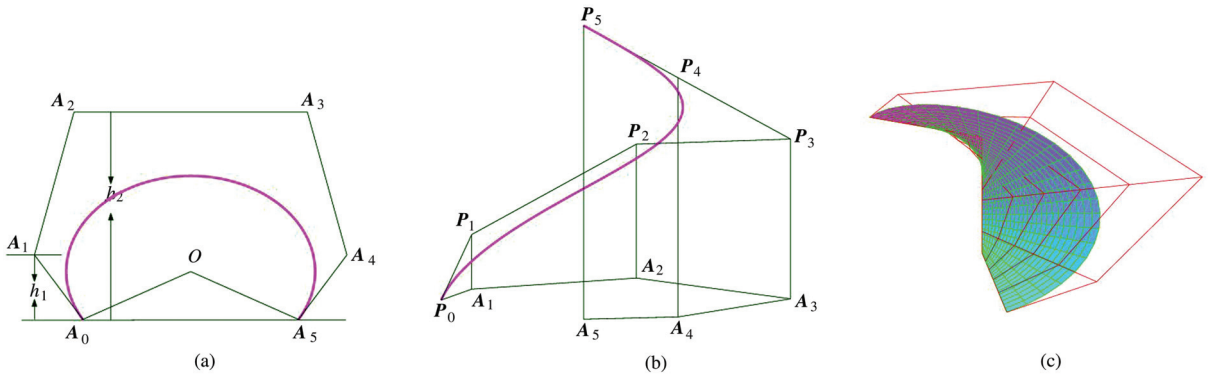

Fig.3. Construction rules of circular arc, helix and right helicoid, $\alpha = 4\pi/3$.

$$\delta = \frac{f_0}{f_1}, \quad L = \frac{h - 2f_1 g + f_0 h}{h},$$
$$M = \frac{g}{h}, \quad N = \frac{h + 2f_1 g - f_0 h}{h},$$
$$s = \sin\alpha, \quad c = \cos\alpha,$$
$$\bar{s} = \sinh\alpha, \quad \bar{c} = \cosh\alpha.$$

In the following, we will present some modeling examples using quintic AHT Bézier basis.

Example 1. *Construction of Circular Arc.*

If $\boldsymbol{A}_0\boldsymbol{A}_1\boldsymbol{A}_2\boldsymbol{A}_3\boldsymbol{A}_4\boldsymbol{A}_5$ is a symmetric hexagon, and $\angle\boldsymbol{A}_1\boldsymbol{A}_0\boldsymbol{A}_5 = \angle\boldsymbol{A}_4\boldsymbol{A}_5\boldsymbol{A}_0 = \alpha/2$, $|\boldsymbol{A}_0\boldsymbol{A}_5| = 2r\sin(\alpha/2)$, $h_1 = r\delta\sin(\alpha/2)$, $h_2 = r(N-1)\cos(\alpha/2) + rM\sin(\alpha/2)$, $|\boldsymbol{A}_2\boldsymbol{A}_3| = r\sqrt{N^2[3-2(c+s)] + 2MN(c-s) + M^2}$, then their corresponding AHT Bézier curve with parametric α represents a circular arc with center angle α and radius r (see Fig.3(a)).

Example 2. *Construction of Helix.*

Step 1. Construct control polygon $\boldsymbol{P}_0\boldsymbol{A}_1\boldsymbol{A}_2\boldsymbol{A}_3\boldsymbol{A}_4\boldsymbol{A}_5$ of the circular arc which has center angle α and radius r on the plane $\boldsymbol{A}$ according to Example 1.

Step 2. Set $\boldsymbol{P}_1\boldsymbol{A}_1 \perp \boldsymbol{A}$, $|\boldsymbol{P}_1\boldsymbol{A}_1| = \omega\delta$; $\boldsymbol{P}_2\boldsymbol{A}_2 \perp \boldsymbol{A}$, $|\boldsymbol{P}_2\boldsymbol{A}_2| = \omega M$; $\boldsymbol{P}_3\boldsymbol{A}_3 \perp \boldsymbol{A}$, $|\boldsymbol{P}_3\boldsymbol{A}_3| = \omega(\alpha - M)$; $\boldsymbol{P}_4\boldsymbol{A}_4 \perp \boldsymbol{A}$, $|\boldsymbol{P}_4\boldsymbol{A}_4| = \omega(\alpha - \delta)$; $\boldsymbol{P}_5\boldsymbol{A}_5 \perp \boldsymbol{A}$, $|\boldsymbol{P}_5\boldsymbol{A}_5| = \omega\alpha$.

Let $\boldsymbol{P}_0\boldsymbol{P}_1\boldsymbol{P}_2\boldsymbol{P}_3\boldsymbol{P}_4\boldsymbol{P}_5$ be the control polygon (see Fig.3(b)). Then the corresponding AHT Bézier curve is the helix with parametric form $\{r\cos t, r\sin t, \omega t\}$, $0 \leqslant t \leqslant \alpha$.

Thus, we can obtain the construction rules of the control mesh of the right helicoid with parametric form $\{a\sinh u\cos v, a\sinh u\sin v, av\}$, $0 \leqslant u \leqslant \alpha$, $0 \leqslant v \leqslant \beta$. Note that $\delta_\alpha, M_\alpha, \delta_\beta, M_\beta$ are defined in (2) corresponding to α and β.

Example 3. *Construction of Right Helicoid.*

Step 1. Construct the control polygon $\boldsymbol{P}_{00}\boldsymbol{P}_{01}\boldsymbol{P}_{02}\boldsymbol{P}_{03}\boldsymbol{P}_{04}\boldsymbol{P}_{05}$ of helix with parametric form $\{a\sinh\alpha\cos v, a\sinh\alpha\sin v, av\}$, $0 \leqslant v \leqslant \beta$, according to the construction rules of helix.

Step 2. Let $\boldsymbol{P}_{50}$ be the center of the circular arc constructed in Example 1, and $\boldsymbol{P}_{55}\boldsymbol{P}_{50} \perp \boldsymbol{A}$, $|\boldsymbol{P}_{55}\boldsymbol{P}_{50}| = a\beta$, $\boldsymbol{P}_{55}, \boldsymbol{P}_{54}, \boldsymbol{P}_{53}, \boldsymbol{P}_{52}, \boldsymbol{P}_{51}, \boldsymbol{P}_{50}$ are collinear, and $|\boldsymbol{P}_{55}\boldsymbol{P}_{54}| = a\delta_\beta$, $|\boldsymbol{P}_{54}\boldsymbol{P}_{53}| = a(M_\beta - \delta_\beta)$, $|\boldsymbol{P}_{53}\boldsymbol{P}_{52}| = a(\beta - 2M_\beta)$, $|\boldsymbol{P}_{52}\boldsymbol{P}_{51}| = a(M_\beta - \delta_\beta)$, $|\boldsymbol{P}_{51}\boldsymbol{P}_{50}| = a\delta_\beta$.

Step 3. Connect $\boldsymbol{P}_{5i}$ and $\boldsymbol{P}_{0i}$. $\boldsymbol{P}_{5i}, \boldsymbol{P}_{4i}, \boldsymbol{P}_{3i}, \boldsymbol{P}_{2i}, \boldsymbol{P}_{1i}, \boldsymbol{P}_{0i}$ are collinear, and $|\boldsymbol{P}_{5i}\boldsymbol{P}_{4i}| : |\boldsymbol{P}_{4i}\boldsymbol{P}_{3i}| : |\boldsymbol{P}_{3i}\boldsymbol{P}_{2i}| : |\boldsymbol{P}_{2i}\boldsymbol{P}_{1i}| : |\boldsymbol{P}_{1i}\boldsymbol{P}_{0i}| = \delta_\alpha : M_\alpha - \delta_\alpha : \alpha - 2M_\alpha : M_\alpha - \delta_\alpha : \delta_\alpha$, $i = 0, 1, 2, 3, 4, 5$. Thus, we can obtain the control mesh representation of right helicoid (see Fig.3(c)).

Example 4. *Construction of Catenary.*

Step 1. Set $|\boldsymbol{P}_0\boldsymbol{A}_4| = a(\bar{c} - 1)$, $\boldsymbol{P}_0, \boldsymbol{A}_1, \boldsymbol{A}_2, \boldsymbol{A}_3, \boldsymbol{A}_4$ are collinear, and $|\boldsymbol{P}_0\boldsymbol{A}_1| = a(L - 1)$, $|\boldsymbol{A}_1\boldsymbol{A}_2| = a(L(\bar{c} - 1) - M\bar{s})$, $|\boldsymbol{A}_2\boldsymbol{A}_3| = a(\bar{c}(1 - L) + \bar{s}(M - \delta))$, $|\boldsymbol{A}_3\boldsymbol{A}_4| = a\delta\bar{s}$.

Step 2. Set $\boldsymbol{P}_1\boldsymbol{P}_0 \perp \boldsymbol{P}_0\boldsymbol{A}_4$, $|\boldsymbol{P}_1\boldsymbol{P}_0| = b\delta$; set $\boldsymbol{P}_2\ \boldsymbol{A}_1 \perp \boldsymbol{P}_0\boldsymbol{A}_4$, $|\boldsymbol{P}_2\boldsymbol{A}_1| = bM$; set $\boldsymbol{P}_3\boldsymbol{A}_2 \perp \boldsymbol{P}_0\boldsymbol{A}_4$, $|\boldsymbol{P}_3\boldsymbol{A}_2| = b(\alpha - M)$; set $\boldsymbol{P}_4\boldsymbol{A}_3 \perp \boldsymbol{P}_0\boldsymbol{A}_4$, $|\boldsymbol{P}_4\boldsymbol{A}_3| = b(\alpha - \delta)$; set $\boldsymbol{P}_5\boldsymbol{A}_4 \perp \boldsymbol{P}_0\boldsymbol{A}_4$, $|\boldsymbol{P}_5\boldsymbol{A}_4| = b\alpha$.

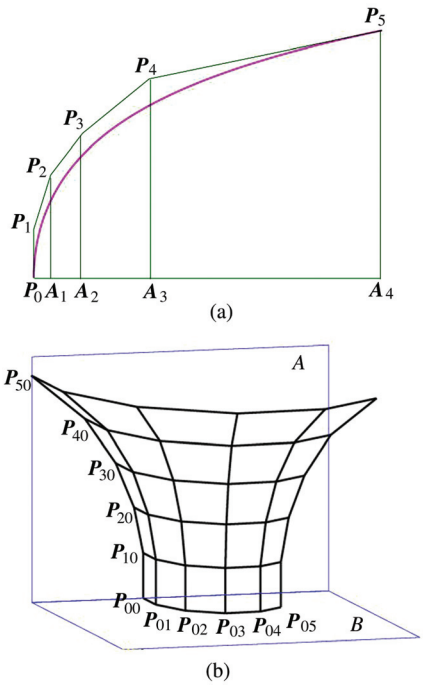

Fig.4. Construction rules of catenary and catenoid, $\beta = 2\pi/3$.

Let $\boldsymbol{P}_0\boldsymbol{P}_1\boldsymbol{P}_2\boldsymbol{P}_3\boldsymbol{P}_4\boldsymbol{P}_5$ be the control polygon (see Fig.4(a)). Then the corresponding AHT Bézier curve is the catenary with parametric form $\{a\cosh t, bt\}$, $0 \leqslant t \leqslant \alpha$.

In the following, we will construct the control mesh of catenoid with parametric form $\{-b\cosh u \sin v, b\cosh u \cos v, bu\}$, $0 \leqslant u \leqslant \alpha$, $0 \leqslant v \leqslant \beta$. Note that $\delta_\alpha, M_\alpha, \delta_\beta, M_\beta$ are defined in (2) corresponding to α and β.

Example 5. *Construction of Catenoid.*

Step 1. Set $A \perp B$, and construct control polygon $\boldsymbol{P}_{00}\boldsymbol{P}_{10}\boldsymbol{P}_{20}\boldsymbol{P}_{30}\boldsymbol{P}_{40}\boldsymbol{P}_{50}$ of catenary with parametric form $\{b\cosh u, bu\}$ on plane A.

Step 2. On the plane B, construct the control polygons of five concentric circular arcs with central angle β, and their radius are b, bL_α, $b(L_\alpha\bar{c} - M_\alpha\bar{s})$, $b(\bar{c} - \delta_\alpha\bar{s})$ and $b\bar{c}$ respectively, and the center of the circular arcs lies on the intersection of the plane A and the plane B. We denote them $\boldsymbol{P}_{00}\boldsymbol{P}_{01}\boldsymbol{P}_{02}\boldsymbol{P}_{03}\boldsymbol{P}_{04}\boldsymbol{P}_{05}$, $\boldsymbol{A}_{i0}\boldsymbol{A}_{i1}\boldsymbol{A}_{i2}\boldsymbol{A}_{i3}$ $\boldsymbol{A}_{i4}\boldsymbol{A}_{i5}$, $i = 2, 3, 4, 5$.

Step 3. Move the control polygons constructed in Step 2 along the normal vector of plane B, such that $\boldsymbol{P}_{00}$ and $\boldsymbol{P}_{10}$ are overlaped, $\boldsymbol{A}_{i0}$ and $\boldsymbol{P}_{i0}$ are overlaped, $i = 2, 3, 4, 5$. So we can obtain five polygons: $\boldsymbol{P}_{i0}\boldsymbol{P}_{i1}\boldsymbol{P}_{i2}\boldsymbol{P}_{i3}\boldsymbol{P}_{i4}\boldsymbol{P}_{i5}$, $i = 1, 2, 3, 4, 5$. Thus, we can obtain the control mesh of the catenoid (see Fig.4(b)).

In the following, we will construct the control mesh of generalized helicoid with parametric form $\{a\sinh u\cos v - b\cosh u\sin v,\ a\sinh u\sin v + b\cosh u\cos v, av + bu\}$, $0 \leqslant u \leqslant \alpha$, $0 \leqslant v \leqslant \beta$.

Example 6. *Construction of Generalized Helicoid.*

Step 1. Construct the control mesh of the right helicoid with parametric form $\{2a\sinh u\cos v, 2a\sinh u\sin v, 2av\}$. We denote the control points by $\boldsymbol{P}^1_{ij}$.

Step 2. Construct the control mesh of the catenoid with parametric form $\{-2b\cosh u\ \cos v, 2b\cosh u\sin v, 2bu\}$. We denote the control points by $\boldsymbol{P}^2_{ij}$.

Step 3. The control points $\boldsymbol{P}_{ij}$ of the generalized helicoid can be obtained by

$$\boldsymbol{P}_{ij} = \frac{1}{2}(\boldsymbol{P}^1_{ij} + \boldsymbol{P}^2_{ij}), \quad i, j = 0, 1, \cdots, 5.$$

Thus, the control mesh is obtained (see Fig.5).

There are many special shapes that can be represented exactly by AHT Bézier basis. For example, in 1855, Bonnet discovered a class of minimal surfaces of which the lines of curvature are planar curves, with parametric forms $\{\frac{\rho u \pm \sin u\cosh v}{\sqrt{1-\rho^2}}, \frac{v \pm \rho\cos u\sinh v}{\sqrt{1-\rho^2}}, \pm\cos u\cosh v\}$, $0 \leqslant u \leqslant \alpha$, $0 \leqslant v \leqslant \beta$. When $\rho = 0$, it is the catenoid; when $\rho \to 1$, it approximates to the Enneper's surface. We can also represent them exactly using the quintic AHT Bézier surfaces (see Fig.6).

5 NUAHT B-Spline Basis

5.1 Non-Uniform Algebraic-Hyperbolic-Trigonometric Spline Space

Let T be a given knot sequence $\{t_i\}_{i=-\infty}^{+\infty}$ with $\Delta t_i = t_{i+1} - t_i \in [0, 3\pi/2)$. We give the definition of algebraic hyperbolic trigonometric spline of order k firstly.

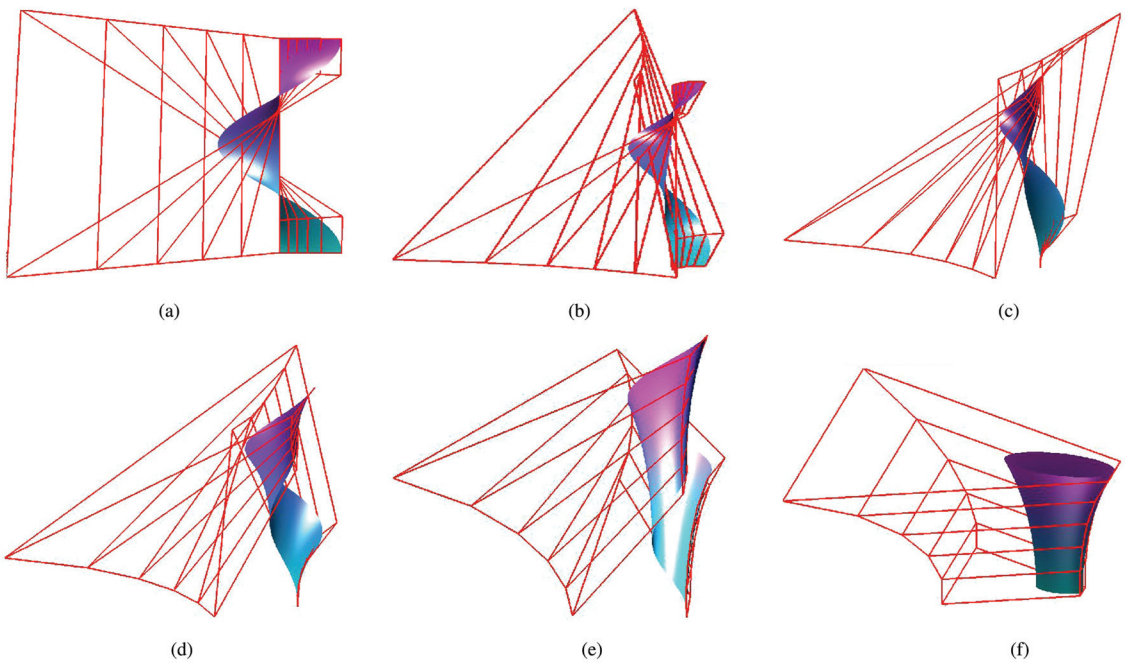

Fig.5. Dynamic deformation from a right helicoid to a catenoid with $\alpha = 1.5$, $\beta = 2\pi$. (a) $a = 1, b = 0$. (b) $a = 0.8, b = 0.2$. (c) $a = 0.6, b = 0.4$. (d) $a = 0.4, b = 0.6$. (e) $a = 0.2, b = 0.8$. (f) $a = 0, b = 1$.

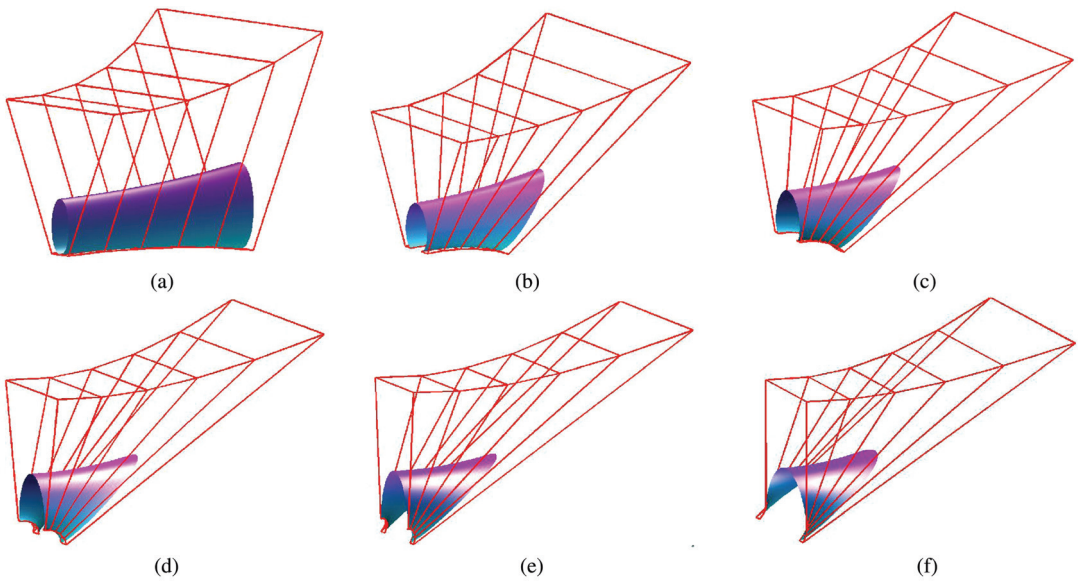

Fig.6. Morphing between catenoid and Enneper's surface with $\alpha = 2\pi, \beta = 1$. (a) $\rho = 0$. (b) $\rho = 0.2$. (c) $\rho = 0.4$. (d) $\rho = 0.6$. (e) $\rho = 0.8$. (f) $\rho = 0.99$.

Definition 5.1 (Algebraic Hyperbolic Trigonometric Spline). *If $s(t)$ is a piecewise function, for each $i = 0, \pm 1, \ldots$, the restriction of $s(t)$ to the subinterval $[t_i, t_{i+1}]$ is in the span of $\{\sin t, \cos t, \sinh t, \cosh t, 1, t, \ldots, t^{k-5}\}$, $k \geqslant 5$, and at a knot t_i of multiplicity r_i, $s(t)$ is $(k - r_i - 1)$ times continuously differential, then we call $s(t)$ an algebraic hyperbolic trigonometric spline of order k.*

Let $\Omega_k[T]$ denote the collection of all algebraic-hyperbolic-trigonometric spline of order k. Furthermore, it can be easily checked that $\Omega_k[T]$ is a linear space. A basis of $\Omega_k[T]$ is called a *non-uniform algebraic-hyperbolic-trigonometric B-splines* (*NUAHT B-spline*) *basis of order k* if the basis functions are non-negative, form a partition of unity, and have minimal support.

5.2 Construction of NUAHT B-Spline Basis

To construct an NUAHT B-spline basis of $\Omega_k[T]$ ($k \geqslant 5$) recursively using integral method, we need to define a set of initial functions $N_{i,4}(t)$ over $\Omega_4[T]$ firstly. $N_{i,4}(t)$ should be piecewise functions and satisfy continuity at the knots $t_i, t_{i+1}, t_{i+2}, t_{i+3}$ and t_{i+4}. Since NUAHT B-spline is a kind of non-uniform spline, $N_{i,4}(t)$ should contain 16 cases of knots listed in the Table 2. To simplify the form of $N_{i,4}(t)$, we will construct $N_{i,4}(t)$ with a unified expression that contains all the 16 cases.

To construct $N_{i,4}(t)$ to satisfy the conditions listed above, we first define l_{i+j}, s_{i+j}, $j = 0, 1, 2, 3, 4$, such that

$$\begin{cases} t_{i+j} = \cdots = t_{i+j+l_{i+j}-1} < t_{i+j+l_{i+j}}, \\ t_{i+j-s_{i+j}} < t_{i+j-s_{i+j}+1} = \cdots = t_{i+j}. \end{cases} \tag{3}$$

Then we define $f(t)$ as follows

$$f(t) = \begin{cases} \frac{1}{2}(\sinh t - \sin t), & t \geqslant 0, \\ 0, & t < 0. \end{cases}$$

Obviously,

$$f(0) = f'(0) = f''(0) = 0,$$
$$f'''(0) = 1, \quad f^{(4)}(t) = f(t).$$

That is, $f^{(i)}(t)$ has a zero of multiplicity $(3 - i)$ at 0, $i = 0, 1, 2, 3$.

Table 2. 16 Cases of Knot
(N is the number of knot intervals between t_i and t_{i+4})

N	Cases of Knot
0	$t_i = t_{i+1} = t_{i+2} = t_{i+3} = t_{i+4}$
1	$t_i < t_{i+1} = t_{i+2} = t_{i+3} = t_{i+4}$, $t_i = t_{i+1} < t_{i+2} = t_{i+3} = t_{i+4}$,
	$t_i = t_{i+1} = t_{i+2} < t_{i+3} = t_{i+4}$, $t_i = t_{i+1} = t_{i+2} = t_{i+3} < t_{i+4}$
2	$t_i < t_{i+1} < t_{i+2} = t_{i+3} = t_{i+4}$, $t_i < t_{i+1} = t_{i+2} < t_{i+3} = t_{i+4}$,
	$t_i < t_{i+1} = t_{i+2} = t_{i+3} < t_{i+4}$, $t_i = t_{i+1} < t_{i+2} < t_{i+3} = t_{i+4}$,
	$t_i = t_{i+1} < t_{i+2} = t_{i+3} < t_{i+4}$, $t_i = t_{i+1} = t_{i+2} < t_{i+3} < t_{i+4}$
3	$t_i < t_{i+1} < t_{i+2} < t_{i+3} = t_{i+4}$, $t_i < t_{i+1} < t_{i+2} = t_{i+3} < t_{i+4}$,
	$t_i < t_{i+1} = t_{i+2} < t_{i+3} < t_{i+4}$, $t_i = t_{i+1} < t_{i+2} < t_{i+3} < t_{i+4}$
4	$t_i < t_{i+1} < t_{i+2} < t_{i+3} < t_{i+4}$

Define

$$f_{i+j}(t) = \begin{cases} f^{(l_{i+j}-1)}(t - t_{i+j}), & 1 \leqslant j + l_{i+j} \leqslant 5, \\ f^{(4-j)}(t - t_{i+j}), & j + l_{i+j} > 5, \end{cases}$$

where l_{i+j} is defined as in (3), $j = 0, 1, 2, 3$. Obviously, $f_{i+j}(t)$ has a zero of multiplicity $(4 - l_{i+j})$ at t_{i+j}.

Let

$$N(t) = \begin{vmatrix} f_i(t_{i+4}) & f_{i+1}(t_{i+4}) & f_{i+2}(t_{i+4}) & f_{i+3}(t_{i+4}) \\ f_i'(t_{i+4}) & f_{i+1}'(t_{i+4}) & f_{i+2}'(t_{i+4}) & f_{i+3}'(t_{i+4}) \\ f_i''(t_{i+4}) & f_{i+1}''(t_{i+4}) & f_{i+2}''(t_{i+4}) & f_{i+3}''(t_{i+4}) \\ f_i(t) & f_{i+1}(t) & f_{i+2}(t) & f_{i+3}(t) \end{vmatrix},$$

define

$$N_{i,4}(t) = \begin{cases} (-1)^{1+s_{i+4}} N(t), & t_i \leqslant t \leqslant t_{i+4}, \\ 0, & \text{otherwise}, \end{cases}$$

where s_{i+4} is defined as in (3).

Thus, we construct a set of desired initial functions $N_{i,4}(t)$. In fact, we have the following theorem.

Theorem 5.1. *$N_{i,4}(t)$ is a piecewise polynomial over T and it has a zero of multiplicity $(4-l_i)$ at t_i, $1 \leqslant l_i \leqslant 4$, it is $(3-l_{i+j})$ times continuously differential at knots t_{i+j}, $1 \leqslant l_{i+j} \leqslant 4$, $j=1,2,3$, and it has a zero of multiplicity $(4-s_{i+4})$ at t_{i+4}, $1 \leqslant l_{i+j} \leqslant 4$.*

From Theorem 5.1, we know that $N_{i,4}(t)$ satisfies our requirement and it contains all the 16 cases of knots listed in Table 2. Note that it has the same continuity at the knots as those of the polynomial B-spline basis of order 4.

For $k \geqslant 5$, $N_{i,k}(t)$ is defined recursively by

$$N_{i,k}(t) = \int_{-\infty}^{t} (\delta_{i,k-1} N_{i,k-1}(s) - \delta_{i+1,k-1} N_{i+1,k-1}(s)) \mathrm{d}s,$$

where $\delta_{i,k} := \left(\int_{-\infty}^{+\infty} N_{i,k}(t) \mathrm{d}t \right)^{-1}$.

From the local support of $N_{i,k}(t)$, which will be listed in Subsection 5.3, we have

$$\int_{-\infty}^{t} \delta_{i,k} N_{i,k}(s) \mathrm{d}s = \begin{cases} 0, & t \leqslant t_i \\ > 0, & t_i < t < t_{i+k}, \\ 1, & t \geqslant t_{i+k}. \end{cases}$$

In particular, in order to ensure that $N_{i,k}$ have the partition of unity property, when $N_{i,k} = 0$, we set $\delta_{i,k} N_{i,k} = 0$ and

$$\int_{-\infty}^{t} \delta_{i,k} N_{i,k}(s) \mathrm{d}s = \begin{cases} 1, & t \geqslant t_{i+k}, \\ 0, & t < t_{i+k}. \end{cases}$$

In fact, $\delta_{i,k} N_{i,k}$ is a Dirac delta function when $N_{i,k} = 0$.

It can be easily seen that $N_{i,k}$ have the properties to be listed in Subsection 5.3, from which we conclude that $N_{i,k}$ constitute a basis of $\Omega_k[T]$, for $k \geqslant 5$. We call $N_{i,k}$ NUAHT B-splines basis of order k, $k \geqslant 5$, $i = 0, \pm 1, \ldots$. Fig.7 illustrates the NUAHT B-spline basis of orders 4 and 5 with the same knot sequence.

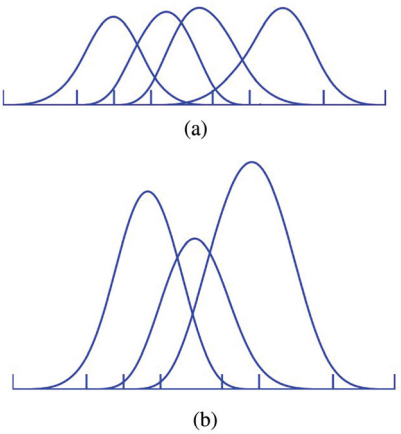

Fig.7. NUAHT B-spline basis of order 4 and order 5 with the same knot sequence. (a) Case of order 4. (b) Case of order 5.

5.3 Properties of the Basis

1) *Differential*: $N_{i,k}$ is $(k - r_j - 1)$ times continuously differential at the knot t_j with r_j the number of times t_j appears in the knot sequence $(t_j)_i^{i+k}$.

2) *Positivity and Local Support*:

$$N_{i,k}(t) \begin{cases} > 0, & t_i < t < t_{i+k}, \\ = 0, & \text{otherwise}. \end{cases}$$

We will prove it in Proposition 5.1.

3) *Zero Function*: $N_{i,k}(t) \equiv 0$ if and only if $t_i = t_{i+1} = \cdots = t_{i+k}$.

4) *Partition of Unity*: $\sum_i N_{i,k}(t) \equiv 1$.

5) *Derivative*: $N'_{i,k}(t) = \delta_{i,k-1} N_{i,k-1}(t) - \delta_{i+1,k-1} N_{i+1,k-1}(t)$. When $N_{i,k-1} = 0$, $\delta_{i,k-1} N_{i,k-1} = 0$.

6) *Linear Independence*: $N_{i,k}(t)$, $i = 0, \pm 1, \ldots$, are linearly independent on $(-\infty, +\infty)$ if the multiplicity of each knot of T is less than $(k+1)$. In particular, $N_{i-k+1,k}(t), \ldots, N_{i,k}(t)$ are linearly independent on $[t_i, t_{i+1}]$ for all i, k with $t_i < t_{i+1}$.

7) Let $r = \max\{s : t_i = t_{i+s}\}$, if $r > k-2$, then we have

$$N_{j,k}(t_i) = \begin{cases} 1, & j = i-1, \\ 0, & j \neq i-1. \end{cases} \tag{4}$$

8) *Relation with AHT Bézier Basis.*

In the case $t_{i-k+1} = t_{i-k+2} = \cdots = t_i < t_{i-k+1} = t_{i-k+2} = \cdots = t_{i+1} = t_{i+2} = \cdots = t_{i+k}$, $N_{i-k+1,k}(t), \ldots, N_{i,k}(t)$ is just the AHT Bézier basis of order k on $[t_i, t_{i+1}]$. From the definitions of the two bases, this property can be proved by induction on k.

Remark 5.1. From this property and property 9) in Subsection 4.1, we can obtain that the distances between knots of the knot vector associated to the NUAHT B-spline basis will increase when k increases.

5.4 Inserting a New Knot

Theorem 5.2. *Let $T := \{t_i\}_{i=-\infty}^{+\infty}$ be a knot sequence, where $t_i \leqslant t_{i+1}$, $i = 0, \pm 1, \pm 2, \ldots$. Inserting a new knot u into T, $t_i \leqslant u < t_{i+1}$, we can obtain a new knot sequence $T^1 : \{t_i^1\}_{i=-\infty}^{+\infty}$. $N_{j,k}(t)$ and $N_{j,k}^1(t)$ are NUAHT B-spline basis functions for the knot sequence T and T^1 respectively. Then we have for all $j, k \geqslant 4$,*

$$N_{j,k}(t) = \alpha_{j,k} N_{j,k}^1(t) + \beta_{j+1,k} N_{j+1,k}^1(t), \tag{5}$$

where for $0 \leqslant r < k$:

$$\alpha_{j,k} = \begin{cases} 1, & j \leqslant i-k, \\ \dfrac{N_{j,k}^{(k-l_j)}(t_j)}{N_{j,k}^{(k-l_j)}(t_j)}, & i-k < j < i-r+1, \\ 0, & j \geqslant i-r+1, \end{cases}$$

$$\beta_{j,k} = \begin{cases} 0, & j \leqslant i-k, \\ \dfrac{N_{j-1,k}^{(k-s_{j+k-1})}(t_{j+k-1})}{N_{j,k}^{(k-s_{j+k-1})}(t_{j+k-1})}, & i-k < j < i-r, \\ 1, & j \geqslant i-r, \end{cases}$$

and for $r \geqslant k$:

$$\alpha_{j,k} = \begin{cases} 1, & j \leqslant i-k+1, \\ 0, & j > i-k+1, \end{cases}$$

$$\beta_{j,k} = \begin{cases} 0, & j \leqslant i-k+1, \\ 1, & j > i-k+1, \end{cases}$$

where l_j *and* s_{j+k-1} *are defined as follows*

$$t_j = \cdots = t_{j+l_{i+j}-1} < t_{j+l_{i+j}};$$
$$t_{j+k-1-s_{j+k-1}} < t_{j+k-s_{j+k-1}} = \cdots = t_{j+k-1},$$

and r *is the multiplicity of the knot* u *in* T. *If* $t_i < u < t_{i+1}$, *then* $r = 0$.

Theorem 5.2 also gives a method to compute the coefficient $\alpha_{j,k}, \beta_{j+1,k}$ for all j. From Theorem 5.2, it is not difficult to show that $\alpha_{i,k} \geqslant 0$, $\beta_{i,k} \geqslant 0$. Furthermore, by the property of partition of unity and the linearly independence of $N^1_{i,k}(t)$, $i = 0, \pm 1, \ldots$, we have the formula $\alpha_{j,k} + \beta_{j,k} = 1$ for all i, k with $N^1_{i,k}(t) \neq 0$ for all i. Then (5) can be rewritten as

$$N_{i,k}(t) = \alpha_{i,k} N^1_{i,k}(t) + (1 - \alpha_{i+1,k}) N^1_{i+1,k}(t). \qquad (6)$$

Now, we give the proof of the non-negativity property of $N_{i,k}(t)$.

Proposition 5.1. $N_{i,k}(t) \geqslant 0$ *for all* t.

Proof. By inserting a series of new knots into knot sequence T such that the multiplicity of each knot t_j is k, we then obtain a new knot sequence denoted by T^1. Let $N^1_{i,k}$ be the new splines with the new knot sequence T^1, then $N_{i,k}(t)$ is a convex combination of $N^1_{i,k}(t)$. By property 8) in Subsection 5.3, we have that $N^1_{i,k}(t)$ determined by t_j is actually an AHT Bézier basis on each interval $[t_j, t_{j+1}]$, $j = i, i+1, \ldots, i+k-1$, $t_j < t_{j+1}$. Thus, we have $N_{i,k}(t) \geqslant 0$ for all t. □

6 NUAHT B-Spline Curves

An NUAHT B-spline curve in $\Omega_k[t_k, t_{n+1}]$ can be defined by

$$\boldsymbol{p}(t) = \sum_{i=1}^{n} N_{i,k}(t) \boldsymbol{P}_i \quad t_k \leqslant t \leqslant t_{n+1}, \qquad (7)$$

where $\boldsymbol{P}_i$ is the control point, $\boldsymbol{P}_1 \boldsymbol{P}_2 \cdots \boldsymbol{P}_n$ is the control polygon. A piece of $\boldsymbol{p}(t)$ over $[t_j, t_{j+1})$ can be written as

$$\boldsymbol{p}(t) = \sum_{i=j-k+1}^{j} N_{i,k}(t) \boldsymbol{P}_i,$$

Fig.8 illustrates two pieces of NUAHT B-spline curves with the same control points but different knot sequences.

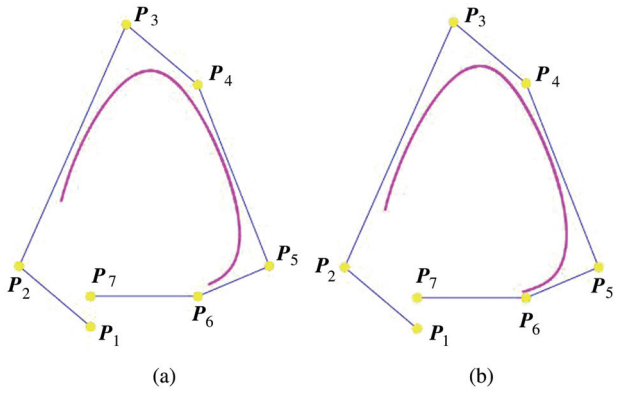

Fig.8. Pieces of NUAHT B-spline curves with the same control points but different knot sequences, $k = 5, n = 7$. (a) Case of uniform knot sequence. (b) Case of non-uniform knot sequence.

6.1 Properties of the Curves

Let $\boldsymbol{p}(t)$ be a piece of NUAHT B-spline curve of order k, then $\boldsymbol{p}(t)$ has the following properties derived directly from the properties of the basis.

1) *Differential*: $\boldsymbol{p}(t)$ is $(k-r-1)$ times continuously differential at knot of multiplicity r.

2) *Convex Hull Property*: $\boldsymbol{p}(t)$ lies inside the convex hull of the corresponding control polygon. It follows from the non-negativity and partition of unity of the NUAHT B-spline basis.

3) *Geometric Invariance*: because $\boldsymbol{p}(t)$ is an affine combination of the control points, its shape is independent of the choice of coordinate system.

4) *Local Control Property*: change of one control point will alter at most k segments of $\boldsymbol{p}(t)$. Hence local adjustment can be made without disturbing the rest of the curve. It is very useful for the interactive design.

5) *Derivative*:

$$\frac{\mathrm{d}}{\mathrm{d}t}\boldsymbol{p}(t) = \sum_{i=j-k+1}^{j+1} \boldsymbol{P}_i^{[1]} N_{i,k-1}(t), \quad t_j \leqslant t < t_{j+1},$$

where $\boldsymbol{P}_i^{[1]} = \delta_{i,k-1} \Delta \boldsymbol{P}_{i-1}$. Furthermore,

$$\boldsymbol{p}^{(r)}(t) = \sum_{i=j-k+1}^{j+r} \boldsymbol{P}_i^{[r]} N_{i,k-r}(t), \quad 0 < r < k-4$$

where $\boldsymbol{P}_i^{[r]} = \delta_{i,k-r} \Delta \boldsymbol{P}_{i-1}^{[r-1]}$, $\Delta \boldsymbol{P}_{i-1} = \boldsymbol{P}_i - \boldsymbol{P}_{i-1}$, $\boldsymbol{P}_0 = \boldsymbol{P}_{n+1} = 0$.

In contrast to the NURBS scheme, the derivative yields a simple curve. Note that $\delta_{i,k-1} N_{i,k-1} = 0$ when $N_{i,k-1} = 0$.

6) *Uniqueness*: if $\boldsymbol{p}(t) = \sum_{i=1}^{n} N_{i,k}(t) \boldsymbol{P}_i = \sum_{i=1}^{n} N_{i,k}(t) \boldsymbol{Q}_i$, we have $\boldsymbol{P}_i = \boldsymbol{Q}_i$. It follows from the linear independence of the NUAHT B-spline basis.

6.2 Subdivision of the Curves

Substituting (6) into (7), we have

$$\begin{aligned}\boldsymbol{p}(t) &= \sum_{i=1}^{n} N_{i,k}(t)\boldsymbol{P}_i \\ &= \sum_{i=1}^{n}(\alpha_{i,k}N^1_{i,k}(t) + (1-\alpha_{i+1,k})N^1_{i+1,k}(t))\boldsymbol{P}_i \\ &= \sum_{i=1}^{n+1} N^1_{i,k}(t)\boldsymbol{P}^1_i,\end{aligned}$$

where

$$\begin{cases} \boldsymbol{P}^1_i = (1-\alpha_{i,k})\boldsymbol{P}_{i-1} + \alpha_{i,k}\boldsymbol{P}_i, \\ \boldsymbol{P}_0 = \boldsymbol{P}_{n+1} = 0. \end{cases} \tag{8}$$

with $N^1_{i,k}$ and $\alpha_{i,k}$ as defined in Subsection 5.4.

According to (8), we can obtain the new control points from the old control points after subdivision. In fact, the process of inserting a new knot is actually a corner cutting process.

If we insert the same knot u, $t_i \leqslant u < t_{i+1}$, iteratively, then from (8) we obtain a series of new control points $\boldsymbol{P}^l_i$, $i = 1, \ldots, n+l$, with l the times of inserting knot. See Fig.9(a).

In particular, when $l = k-1$, from (4), we can obtain

$$N^l_{j,k}(u) = \begin{cases} 1, & j = i, \\ 0, & j \neq i, \end{cases}$$

then,

$$\boldsymbol{p}(u) = \sum_{j=0}^{n+l} \boldsymbol{P}^l_j N^l_{j,k}(u) = \boldsymbol{P}^l_i.$$

To simplify notation, we use $T^r = \{t^r_i\}^{+\infty}_{i=-\infty}$ to denote a new knot sequence obtained by inserting a series of new knots into the initial knot sequence $T = \{t_i\}^{+\infty}_{i=-\infty}$, where r is the times of inserting knots. Thus, the initial control polygon $\boldsymbol{P}_1\boldsymbol{P}_2\cdots\boldsymbol{P}_n$ changes to $\boldsymbol{P}^r_1\boldsymbol{P}^r_2\cdots\boldsymbol{P}^r_{n+r}$. And let $\Delta^r = \max|t^r_{i+1} - t^r_i|$, $i = 1, \ldots, n+k+r-1$. We have the following theorem.

Theorem 6.1. *If* $\lim_{r\to+\infty}\Delta^r = 0$, *then the sequence of the control polygons* $\boldsymbol{P}^r_1\boldsymbol{P}^r_2\cdots\boldsymbol{P}^r_{n+r}$ *converges to the spline curve* $\boldsymbol{p}(t)$.

Its proof is very similar with the case of NUAT B-spline curves[16]. Theorem 6.1 ensures that recursive subdivision of control polygon leads to its corresponding NUAHT B-spline curve. With this theorem, the variation diminishing property and the convexity preserving property of NUAHT B-spline curve can be easily deduced. Since AHT Bézier curve is a special case of AHT B-spline curve, we can easily obtain that AHT Bézier curves also have the above two properties.

Similarly, we can obtain the de Casteljau-type algorithm of AHT Bézier curves via inserting new knots. That is, supposing that $\boldsymbol{p}(t)$ is an AHT Bézier curve of order k defined on $[0, \alpha]$, we first consider $\boldsymbol{p}(t)$ as a piece of NUAHT B-spline curve with knot sequence $T = [\underbrace{0, \ldots, 0}_{k}, \underbrace{\alpha, \ldots, \alpha}_{k}]$. Then, we insert new knot $u \in [0, \alpha]$ into knot sequence T such that the multiplicity of u is $(k-1)$. Thus, we obtain $\boldsymbol{p}(u)$, $u \in [0, \alpha]$. Fig.9(b) shows the subdivision of AHT Bézier curve of order 5.

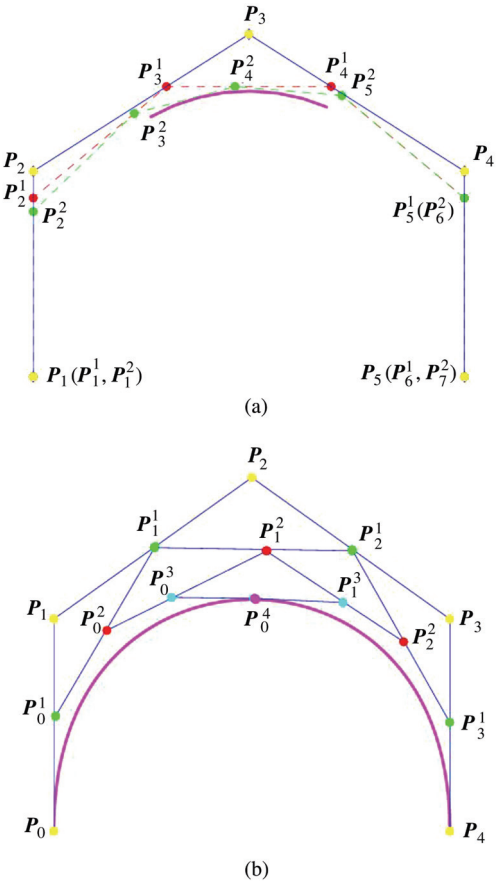

Fig.9. Subdivision of the curves. (a) Subdivision of AHT B-spline curve of order 5. (b) Subdivision of AHT Bézier curve of order 5.

6.3 Some Examples

In this subsection, we will give some examples constructed by the NUAHT B-spline curves. In particular, we can represent the conics and some transcendental curves using only one control polygon. This is very useful for constructions of 2D-profiles in engineering design. Using two ellipses and a part of hyperbola, we construct a curve in Fig.10(a), which is similar to the profile of the head of the sheep. The profile of the vase is constructed in Fig.10(b). In Fig.10(c), we construct the profile of the table tennis racket using an ellipse.

6.4 NUAHT B-Spline Surface

Exactly as in the construction of B-spline tensor product surface from B-spline curve, we can construct NUAHT B-spline surface from NUAHT B-spline curve

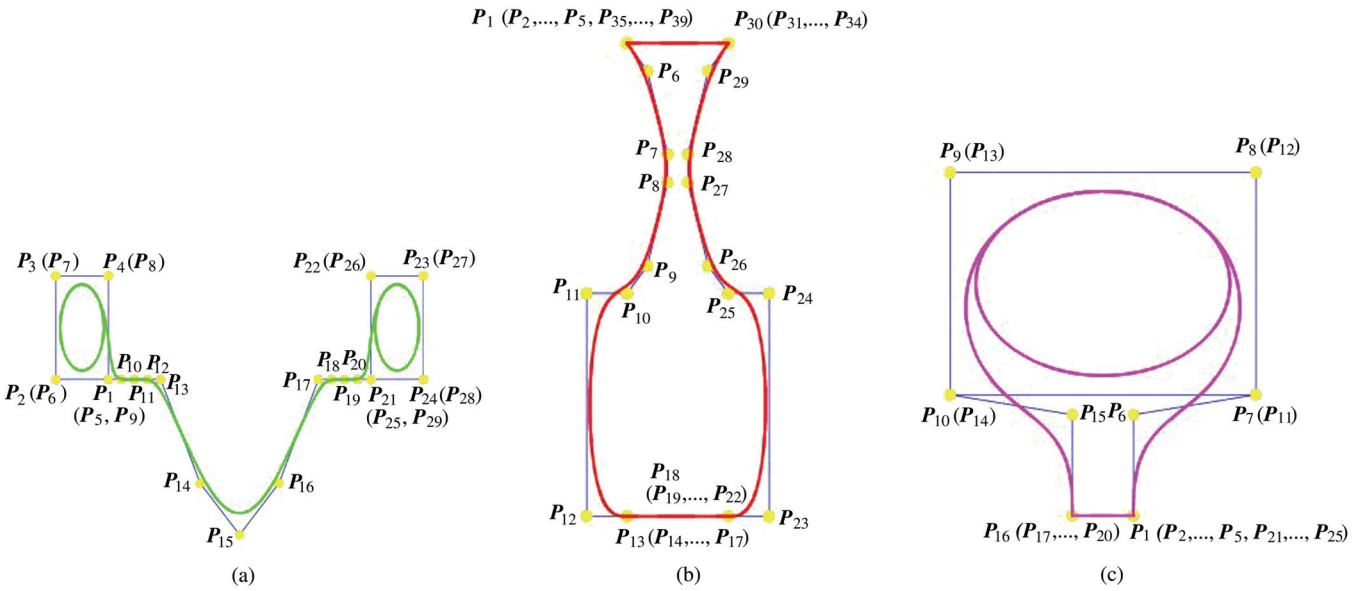

Fig.10. Some 2-D profiles constructed by AHT B-spline curves. (a) Head of the sheep. (b) Vase. (c) Table tennis racket.

by

$$\boldsymbol{p}(u,v)=\sum_{i=1}^{n}\sum_{j=1}^{m}N_{i,k}(u)N_{j,h}(v)\boldsymbol{P}_{i,j},$$

where $\boldsymbol{P}=[\boldsymbol{P}_{i,j}]$ is the control mesh, $u\in[t_k,t_{n+1}]$, $v\in[t_h,t_{m+1}]$; $n\geqslant k, m\geqslant h$. Its properties can be deduced by those of NUAHT B-spline curve.

7 Conclusion

In this paper, we have proposed two new kinds of curves, which are generated over the space $\mathrm{span}\{\sin t,\cos t,\sinh t,\cosh t,1,t,\ldots,t^{n-5}\}$. These two kinds of curves not only inherit the advantage of polynomial curves, but also take on the characteristics of trigonometric functions and hyperbolic functions. That is, in addition to the polynomial curves, they also provide exact representations of conics. Hence, similar with the rational Bézier scheme and the NURBS scheme, they are also unified mathematics models of polynomial curves and conics.

In particular, the new curves are more stable in calculation than the rational schemes[27]. Furthermore, we can achieve for the straight line, circle and helix an arc-length parameterization by the new curves, but the rational schemes cannot. More important, the new curves can afford exact representation of remarkable transcendental curves, such as the helix, the cycloid and the catenary, but the rational models cannot. Therefore, we expect that the new models can be employed as new powerful tools for constructing freeform curves and surfaces in CAGD.

References

[1] Lee J, Park H. Geometric properties of ribs and fans of a Bézier curve. *Journal of Computer Science and Technology*, 2006, 21(2): 279~283.

[2] He Y, Gu X, Qin H. Automatic shape control of triangular B-splines of arbitrary topology. *Journal of Computer Science and Technology*, 2006, 21(2): 232~237.

[3] Li G, Li H. Blending parametric patches with subdivision surfaces. *Journal of Computer Science and Technology*, 2002, 17(4): 498~506.

[4] Farin G. Curves and Surfaces for CAGD. 5th Edition, Morgan Kaufmann, 2002.

[5] Farin G. NURB Curves and Surfaces: From Projective Geometry to Practical Use. 2nd Edition, Wellesley, MA: AK Peters,1999.

[6] Piegl L, Tiller W. The NURBS Book. 2nd Edition, Springer, 1997.

[7] Farin G. Rational Curves and Surfaces. Mathematical Methods in Computer Aided Geometric Design, Lyche T, Schumaker L (eds.), Boston: Kluwer, Academic Press, 1989.

[8] Farin G. From conics to NURBS: A tutorial and survey. *IEEE Computer Graphics and Applications* , 1992, 12(5): 78~86.

[9] Piegl L. On NURBS: A survey. *IEEE Computers Graphics and Applications*, 1991, 11(1): 55~71.

[10] Peña J. Shape preserving representations for trigonometric polynomial curves. *Computer Aided Geometric Design*, 1997, 14(1): 5~11.

[11] Zhang J. C-curves: An extension of cubic curves. *Computer Aided Geometric Design*, 1996, 13(3): 199~217.

[12] Zhang J. Two different forms of C-B-splines. *Computer Aided Geometric Design*, 1997, 14(1): 31~41.

[13] Pottmann H, Wagner M. Helix splines as example of affine Tcheby-cheffian splines. *Advance in Computational Mathematics*, 1994, 2(1): 123~142.

[14] Sânchez-Reyes J. Harmonic rational Bézier curves, p-Bézier curves and trigonometric polynomials. *Computer Aided Geometric Design*, 1998, 15(9): 909~923.

[15] Mainar E, Peña J, Sánchez-Reyes J. Shape preserving alternatives to the rational Bézier model. *Computer Aided Geometric Design*, 2001, 18(1): 37~60.

[16] Li Y, Wang G. Two kinds of B-basis of the algebraic hyperbolic space. *Journal of Zhejiang University*, 2005, 6A(7): 750~759.

[17] Lü Y, Wang G, Yang X. Uniform hyperbolic polynomial B-spline curves. *Computer Aided Geometric Design*, 2002, 19(6): 379~393.

[18] Chen Q, Wang G. A class of Bézier-like curves. *Computer Aided Geometric Design*, 2003, 20(1): 29∼39.
[19] Wang G, Chen Q, Zhou M. NUAT B-spline curves. *Computer Aided Geometric Design*, 2004, 21(2): 193∼205.
[20] Zhang J, Krause F, Zhang H. Unifying C-curves and H-curves by extending the calculation to complex numbers. *Computer Aided Geometric Design*, 2005, 22(9): 865∼883.
[21] Zhang J, Krause F. Extend cubic uniform B-splines by unified trigonometric and hyperbolic basis. *Graphic Models*, 2005, 67(2): 100∼119.
[22] Carnicer J, Peña J. Totally positive for shape preserving curve design and optimality of B-splines. *Computer Aided Geometric Design*, 1994, 11(6): 635∼656.
[23] Peña J. Shape Preserving Representations in Computer Aided Geometric Design. Commack, New York: Nova Science Publishers, 1999.
[24] Dong C, Wang G. On convergence of the control polygons series of C-Bézier curves. In *Proc. Geometric Modeling and Processing*, Beijing, April 13∼15, 2004, pp.49∼55.
[25] Mainar E, Peña J. Corner cutting algorithms associated with optimal shape preserving representations. *Computer Aided Geometric Design*, 1999, 16(9): 883∼906.
[26] Carnicer J, Mainar E, Peña J. Critical length for design purposes and Extended Chebyshev spaces. *Constructive Approximation*, 2004, 20(1): 55∼71.
[27] Mainar E, Peña J, Sanchez-Reyes J. Shape preserving alternatives to the rational Bézier model. *Computer Aided Geometric Design*, 2001, 18(1): 37∼60.

Gang Xu is a Ph.D. candidate of Zhejiang University in applied mathematics. He received his B.S. degree in computational mathematics from Shandong University in 2003. His main research interests include geometric design and computation, digital geometry processing and image processing.

Guo-Zhao Wang is a professor of applied mathematics in Zhejiang University. His main research interests include computer aided geometric design, computer graphics and medical image processing.